PLANT SCIENCE TODAY
Vol 13(sp1): 1-8
https://doi.org/10.14719/pst.12819

eISSN 2348-1900

RESEARCH ARTICLE

A rapid, high-throughput, non-invasive approach for assessing drought tolerance in rose (*Rosa* spp.) using RGB-derived vegetation indices

Chaitra K[1], Namita[1*], Sudhir Kumar[2*], M K Singh[1], Sapna Panwar[1], Chellapilla Bharadwaj[3], Amitha Mithra Sevanthi[4], Bhupinder Singh[5], Rajasekar Raman[2] & Vikram[6]

[1]Department of Floriculture and Landscaping, ICAR-Indian Agricultural Research Institute, New Delhi 110 012, India
[2]Department of Plant Physiology, ICAR-Indian Agricultural Research Institute, New Delhi 110 012, India
[3]Department of Genetics and Plant Breeding, ICAR-Indian Agricultural Research Institute, New Delhi 110 012, India
[4]Department of Molecular Biology and Biotechnology, ICAR-Indian Agricultural Research Institute, New Delhi 110 012, India
[5]Department of Environment Science, ICAR-Indian Agricultural Research Institute, New Delhi 110 012, India
[6]Department of Seed Science and Technology, ICAR-Indian Agricultural Research Institute, New Delhi 110 012, India

*Correspondence email - namita.icar@gmail.com, sudhirnpf@gmail.com

Received: 19 November 2025; Accepted: 23 February 2026; Available online: Version 1.0: 08 April 2026

Cite this article: Chaitra K, Namita, Sudhir K, Singh MK, Sapna P, Chellapilla B, Amitha MS, Bhupinder S, Rajasekar R, Vikram. A rapid, high-throughput, non-invasive approach for assessing drought tolerance in rose (*Rosa* spp.) using RGB-derived vegetation indices. Plant Science Today. 2026; 13(sp1): 1-8. https://doi.org/10.14719/pst.12819

Abstract

Drought stress poses a significant threat to rose (*Rosa* spp.) cultivation, impacting plant vigor, floral quality and marketability. Traditional drought screening methods are often destructive and labor-intensive, limiting their application in large-scale breeding programs. This study presents a non-destructive and high-throughput phenotyping approach for assessing drought responses in rose using RGB-derived vegetation indices (VIs) obtained from multi-angle imaging. Twenty-eight diverse rose genotypes were evaluated under well-watered (WW) and induced drought (ID) conditions using a LemnaTec Scanalyzer 3D platform. A total of 56 indices from side-view (SV) and top-view (TV) images were computed to quantify canopy color, greenness and pigment-related traits. Analysis of variance revealed significant genotypic differences and strong genotype × treatment (G × T) interactions across most indices, demonstrating their sensitivity to drought-induced physiological changes. Multivariate analyses, including Principal Component Analysis (PCA) and Pearson correlation matrix evaluation, were performed to explore trait relationships and identify key traits associated with drought stress. These analyses effectively differentiated greenness-related and stress-responsive traits. In addition, the MGIDI analysis integrated all indices and identified 'Queen Elizabeth', 'Jwala', *Rosa chinensis*, 'Sylvia' and 'Rose Sherbet' as the top-performing drought-tolerant genotypes. Integration of leaf wilting scores validated the reliability of these indices as accurate indicators of drought response, with tolerant genotypes exhibiting lower LWS and higher greenness indices. Overall, the study demonstrates that RGB-based high-throughput phenotyping provides a rapid, efficient and scalable method for drought tolerance assessment in roses, offering a valuable tool for accelerating selection in ornamental breeding programs.

Keywords: Drought stress; high-throughput phenotyping; leaf wilting score; RGB-derived vegetation indices; rose

Introduction

Rose (*Rosa* spp.) is one of the most important ornamental plants globally, valued for its beauty, fragrance, cultural symbolism and economic significance in the cut flower, landscaping and perfumery industry. It accounts for over 35 % of the global cut flower market, with major production centers in the Netherlands, Kenya, Colombia and Ecuador (1). The genus *Rosa* is highly diverse, comprising more than 150 species and thousands of cultivars adapted to varied agro-climatic conditions (2). Breeding programs have traditionally emphasized ornamental traits such as flower size, color, fragrance and vase life (3). However, the increasing frequency and severity of drought under climate change now pose serious challenges to sustainable rose production (4, 5).

Drought is one of the most detrimental abiotic stresses, particularly under changing climatic conditions and increased water constraints. In roses, drought stress negatively affects several key aspects of plant development, including leaf expansion, shoot elongation, flower initiation and bud development. These physiological changes result in reduced plant vigor and a marked decline in visual appeal. Furthermore, drought often causes reductions in flower size, number and color intensity, which adversely impact both the aesthetic value and postharvest performance of roses (6-8). Conventional drought screening methods, such as assessing relative water content (RWC), chlorophyll levels, or biomass, are often destructive and labor-intensive, making them unsuitable for large-scale screening programs. Therefore, developing rose varieties with improved drought tolerance has become a high-priority objective in modern breeding programs.

Advances in high-throughput phenotyping (HTP) platforms have enabled rapid, non-destructive monitoring of plant responses to environmental stresses (9–11). These systems monitor plant health using various imaging modalities including thermal, hyperspectral, fluorescence, LiDAR and RGB. Among these, RGB (red-green-blue) imaging is recognized for its low cost, ease of use and ability to capture a wide range of morphological and physiological traits. RGB images reflect visible wavelengths from plant canopies, enabling the extraction of color-related features. They have been widely applied to estimate morphological traits (12), physiological status (13), and both biotic (14) and abiotic stresses (15–18). Multi-angle imaging, including side-view (SV) and top-view (TV) perspectives, provides a more comprehensive representation of plant architecture and enhances the accuracy of detecting stress-induced growth changes. Beyond basic morphometric traits, RGB images allow the computation of vegetation indices (VIs), which are mathematical combinations of red, green and blue pixel values that enhance the detection of physiological stress by amplifying subtle changes in leaf coloration. Although RGB-based phenotyping has been widely applied in major crops such as maize, wheat, rice and soybean, its use in ornamental breeding, particularly roses, remains limited.

Therefore, the objective of this study was to evaluate drought-responsive variation in 28 rose genotypes using RGB-derived vegetation indices obtained from multi-angle imaging and to identify drought-tolerant genotypes by integrating RGB-based phenotyping with multivariate analyses and validating their performance using leaf wilting scores.

Materials and Methods

Experimental site and plant material

The experiment was conducted at the Nanaji Deshmukh Plant Phenomics Centre, ICAR (Indian Agricultural Research Institute), New Delhi, India (28.641999° N, 77.161° E) during 2023–2024. Twenty-eight rose genotypes (Table 1) were selected for drought stress evaluation based on genetic diversity, contrasting morphological characteristics and availability in the departmental germplasm collection, ensuring representation of both modern hybrid teas and wild species with potential adaptive variability under water-limited conditions. Plants were propagated using semi-hardwood stem cuttings and established in nursery beds. After rooting, healthy and uniform plants were transplanted into white phenomics pots (0.19 m diameter × 0.40 m height) filled with 12 kg of homogenized sandy loam soil with a pH of 6.78 and an electrical conductivity (EC) of 0.82 dS m^{-1}.

Growth conditions and drought treatments

During the establishment phase, plants were grown under natural field conditions, with average daytime temperatures of 28–30 °C and relative humidity of 60–70 %. During this phase, all plants were irrigated uniformly to maintain optimum soil moisture conditions, ensuring proper plant establishment before the imposition of drought stress. A foliar spray of balanced NPK (19:19:19) at 5 g L^{-1} along with a micronutrient mixture at 0.5 g L^{-1} was applied every 15 days to ensure adequate nutrient supply throughout the growth and developmental phases. For stress imposition, plants were transferred to a controlled greenhouse and subjected to two irrigation regimes: (i) well-watered (WW) where soil moisture was maintained at 80 ± 5 % of field capacity (FC) through regular irrigation and (ii) induced drought (ID), where irrigation was withheld, allowing soil moisture to gradually decline to 10 ± 5 % of FC over a period of 30 days. Soil moisture content was periodically monitored using the gravimetric method to maintain the target moisture levels across treatments. Standard pest and disease management practices were followed throughout the experiment.

Image acquisition and processing

Phenotypic data were collected using a LemnaTec Scanalyzer 3D platform (LemnaTec GmbH, Aachen, Germany). RGB images were captured using a Prosilica GT6600 RGB camera equipped with an ON -Semi KAI-29050 sensor. Each plant was imaged from multi-angles, including a top view (TV) and three side views (SV) at 0°, 120° and 240°, to ensure comprehensive characterization of plant architecture. The imaging chamber was standardized with uniform lighting and a white background to improve segmentation accuracy. Imaging was carried out at the end of the drought stress period, with all plants imaged on the same day and within the same time window (10:00–12:00 h) to minimize diurnal variation. Image processing was performed using LemnaGrid software. Background segmentation was carried out using threshold-based methods to isolate plant pixels and quantitative traits and color features were extracted from the plant area. The processed data were exported in CSV format for further statistical analysis.

RGB-derived vegetation indices

From the processed RGB images, 28 vegetation indices (Table 2) were calculated for both TV and SV, resulting in a total of 56 RGB-derived vegetation indices. These included basic color channels (R, G, B), ratio indices (RGRI, RBRI, GBRI), normalized indices (r, g, b), intensity (INT), channel difference indices (RMGI, RMBI, GMBI), channel difference ratio indices (RGVI, RBVI, GBVI), normalized difference indices (NRGI, NRBI, NGBI), excess indices (ExR, ExG), advanced indices (MGRVI, RGBVI, VARI), gray value and principal component–based indices (PCA1, PCA2, IPCA). These indices were selected based on previous studies for their effectiveness in capturing variation in pigmentation, chlorophyll concentration and canopy health under stress.

Table 1. List of rose genotypes utilized in the present study

Code	Genotype	Code	Genotype	Code	Genotype	Code	Genotype
G-1	Pusa Alpana	G-8	*Rosa multiflora*	G-15	Dr. B. P. Pal	G-22	*Rosa chinensis* Viridiflora
G-2	Taj Mahal x Oklahoma (RH-03-2017)	G-9	Summer Snow	G-16	Bewitched	G-23	Queen Elizabeth
G-3	Pasadena x Midas Touch (RH-1-2019)	G-10	Pink Parfait	G-17	*Rosa glutinosa*	G-24	Jwala
G-4	*Rosa bourboniana*	G-11	*Rosa indica* Major	G-18	Happiness	G-25	*Rosa slancensis*
G-5	*Rosa tomentosa*	G-12	*Rosa brunonii*	G-19	Folklore	G-26	*Rosa chinensis*
G-6	*Rosa moschata*	G-13	Delhi White Pearl	G-20	Rani Sahiba	G-27	Rose Sherbet
G-7	Pusa Lakshmi	G-14	White Queen Elizabeth	G-21	Sylvia	G-28	Pusa Virangana

Table 2. RGB-derived vegetation indices for both side view (SV) and top view (TV)

Abbreviation	Index	Formula	Reference
R	Red Channel	R	
G	Green Channel	G	
B	Blue Channel	B	
RGRI	Red Green Ratio Index	R/G	(20)
RBRI	Red Blue Ratio Index	R/B	(21)
GBRI	Green Blue Ratio Index	B/G	(22)
r / NRI	Normalized Red Index	R/(R+G+B)	
g / NGI	Normalized Green Index	G/(R+G+B)	(23)
b / NBI	Normalized Blue Index	B/(R+G+B)	
INT	Color Intensity	(R + G + B)/3	(24)
RMGI	Red Minus Green Index	R−G	
RMBI	Red Minus Blue Index	R−B	
GMBI	Green Minus Blue Index	G−B	
RGVI	Red Green Vegetation Index	(R-G) / (R+G)	
RBVI	Red Blue Vegetation Index	(R-B) / (R+B)	(25)
GBVI	Green Blue Vegetation Index	(G-B) / (G+B)	
NRGI	Normalized Red-Green Index	(R-G)/(R+G+B)	
NRBI	Normalized Red-Blue Index	(R-B)/(R+G+B)	
NGBI	Normalized Green-Blue Index	(G-B)/(R+G+B)	
ExR	Excess Red Vegetation Index	1.4r - g	(26, 27)
ExG	Excess Green Vegetation Index	2g – r – b	(28)
PCA 1	Principal Component Analysis 1	-0.977b + 0.916((G-B)/(G + B)) + 0.995((R-B)/(R + B)) + 0.771((R-G)/(R + G))	(29)
PCA 2	Principal Component Analysis 2	0.999|R-B| + 0.92|G-B| + 0.886|R-G|	
I_{PCA}	Principal Component Analysis Index	0.994*|R – B|+ 0.961*|G – B|+ 0.914*|G – R|	(30)
MGRVI	Modified Green Red Vegetation Index	$(G^2 – R^2) / (G^2 + R^2)$	(31)
RGBVI	Red Green Blue Vegetation Index	$(G^2 – (B \times R)) / (G^2 + (B \times R))$	
VARI	Visible Atmospherically Resistant Index	(G – R) / [(G + R) – B]	(32)
Gray	Gray value	0.2898R + 0.5870G + 0.1140B	(33)

Leaf wilting score assessment

Leaf Wilting Score (LWS) was used to visually assess drought-induced stress using a standardized 0–5 scale (19). A score of 0 indicated a healthy plant with no visible wilting; 1 indicated a minor folding of terminal or young leaves with the overall plant appeared healthy. A score of 2 indicated considerable folding in most leaves, including older ones showing early wilting indications. At score 3, all leaves were wilted or drooped, with older foliage showing the most severe symptoms. Score 4 described total wilting, chlorophyll degradation-induced leaf discolouration and early leaf drying. A score of 5 indicated extreme wilting and yellowing of all leaves, with more than half of the foliage dry and crisp, indicating that the plant was close to physiological death. Wilting scores were recorded at the end of the drought period for all genotypes and treatments and assessments were conducted at the same time of day (10:00–12:00 h) to minimize subjectivity and diurnal fluctuations in wilting symptoms.

Statistical analysis

Statistical analysis was performed using R software (version 4.5.1). The experiment was conducted using three biological replicates per genotype per treatment and mean values were used for subsequent analyses. Analysis of variance (ANOVA) was conducted to evaluate the effects of genotype, treatment and genotype × treatment interactions on RGB-derived vegetation indices, with significance set at $p < 0.05$. Pearson's correlation coefficients were computed to examine interrelationships among indices. Principal Component Analysis (PCA) was performed on standardized RGB-derived vegetation indices to reduce dimensionality and summarize major patterns of trait variation across moisture regimes. The Multi-Trait Genotype–Ideotype Distance Index (MGIDI) was calculated to rank genotypes for drought resilience by integrating multiple trait performances into a single metric.

Results

Genotypic variation of RGB-derived vegetation indices

Significant variation was observed among the 28 rose genotypes for all RGB-derived indices obtained from both side view (SV) and top view (TV) imaging under induced drought (ID) and well-watered (WW) conditions (Supplementary Tables 1 and 2). In the SV images, a highly significant genotype × treatment (G × T) interaction ($p<0.001$) were observed for most basic RGB channels (R_SV, G_SV, B_SV) and their derived indices, including RGRI_SV, RBRI_SV, r_SV, g_SV, INT_SV, RMGI_SV, RMBI_SV, GMBI_SV, RGVI_SV, RBVI_SV, NRGI_SV, NRBI_SV, ExR_SV, ExG_SV, PCA1_SV, PCA2_SV, IPCA_SV, MGRVI_SV, RGBVI_SV, VARI_SV and Gray_SV, indicating strong genotype-specific responses across treatments. Moderate significance ($p < 0.01$) was recorded for NGBI_SV, while GBRI_SV, GBVI_SV and b_SV showed lower but still significant interactions ($p \leq 0.05$), reflecting comparatively weaker sensitivity to treatment effects when captured from the side-view.

Similarly, in the TV images, most RGB-derived indices exhibited highly significant ($p < 0.001$) G × T interaction effects, confirming substantial genotypic variability in basic RGB color and derived indices under contrasting moisture regimes. Only RBRI_TV, RBVI_TV, NRBI_TV and PCA 1_TV showed moderate significance ($p < 0.01$), while all other indices including R_TV, G_TV, B_TV, RGRI_TV, GBRI_TV, r_TV, g_TV, b_TV, INT_TV, RMGI_TV, RMBI_TV, GMBI_TV, RGVI_TV, GBVI_TV, NRGI_TV, NGBI_TV, ExR_TV, ExG_TV, PCA2_TV, IPCA_TV, MGRVI_TV, RGBVI_TV, VARI_TV and Gray_TV were highly significant.

Multivariate analyses

Principal component analysis (PCA)

PCA was performed to reduce dimensionality and explore trait patterns under WW and ID conditions. The first two components, PC1 and PC2, explained 48.4 % and 45.4 % of the total variation,

respectively. The PCA biplot (Fig. 1) revealed a clear grouping of indices based on spectral behavior and physiological relevance. Indices such as ExG, g, RGBVI, Gray, GBVI, VARI, MGRVI, NGBI, RGVI, NRGI and RMGI loaded strongly on PC1 and were associated with plant greenness and vigor, especially under drought condition. In contrast, indices including RGRI, RMBI, R, ExR, r, NRBI, RBRI, RBVI, b, GBRI, INT and B aligned along PC2, representing traits linked to stress-induced reflectance changes and pigment degradation. Indices such as PCA-derived indices (PCA1, PCA2, IPCA) and GMBI showed intermediate loadings, indicating their ability to capture transition patterns between healthy and stressed conditions. Overall, PCA effectively differentiated drought-responsive features, facilitating the identification of key indices for stress phenotyping.

Pearson correlation analysis

Pearson's correlation matrix (Fig. 2) revealed strong positive correlations ($r > 0.80$) among greenness-related indices such as RMGI, RGVI, NRGI, MGRVI, VARI, RGBVI, g and ExG, indicating their shared physiological basis associated with chlorophyll content and overall plant health. In contrast, indices such as r, b, GBRI, RGRI and ExR exhibited strong negative correlations ($r < -0.70$), reflecting their sensitivity to red and blue reflectance during stress condition.

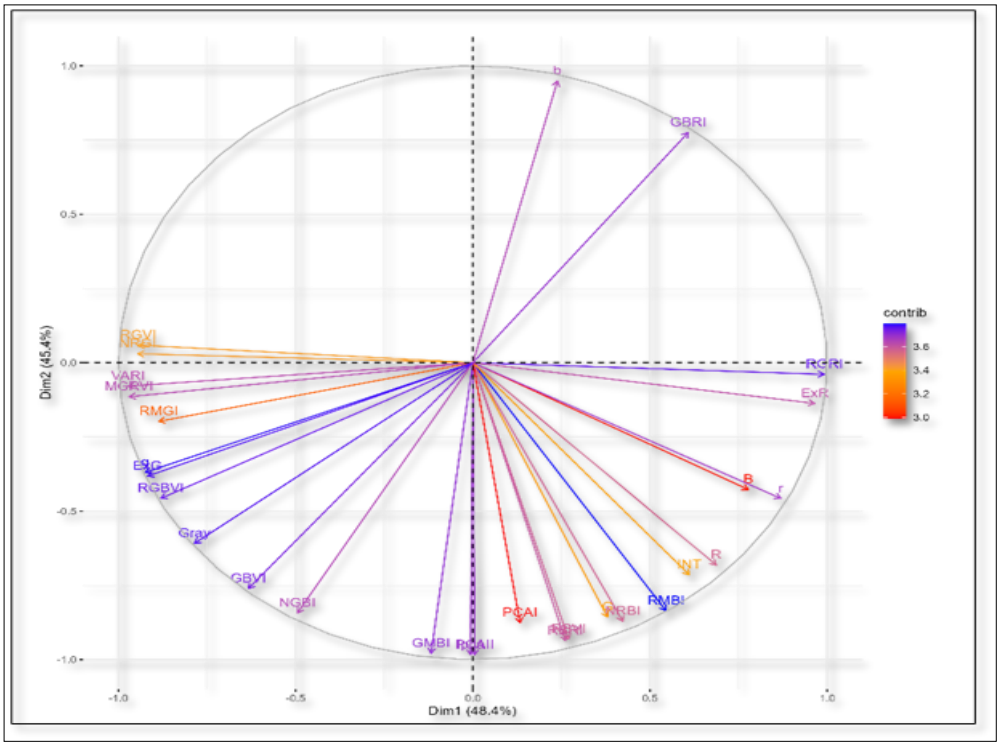

Fig. 1. Principal Component Analysis (PCA) biplot illustrating the contribution of RGB-derived vegetation indices under well-watered (WW) and induced drought (ID) conditions.

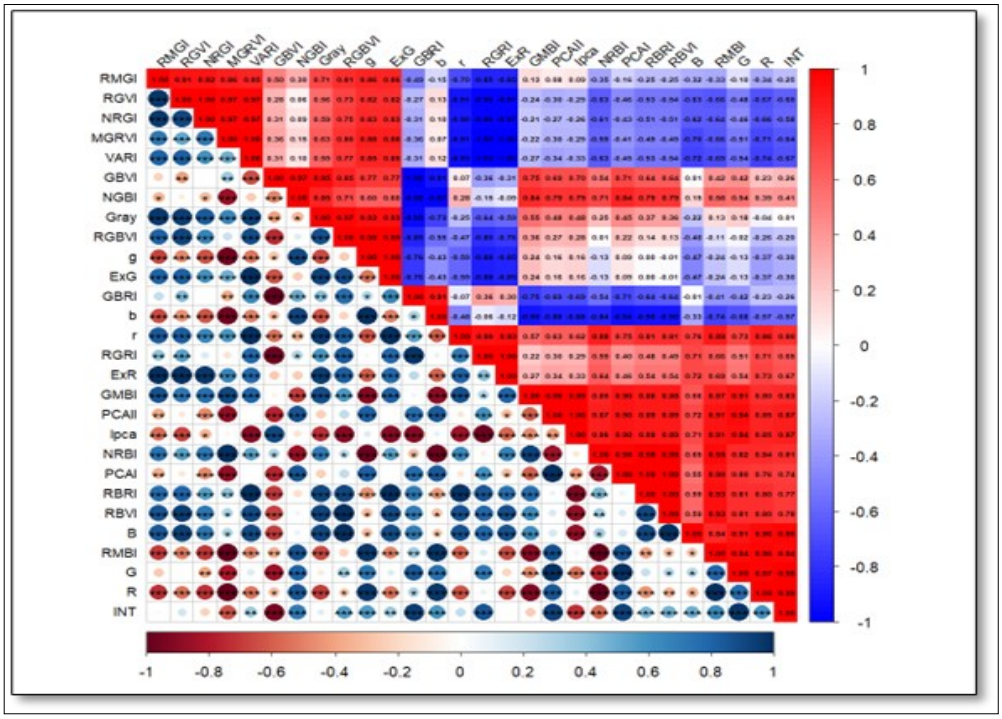

Fig. 2. Pearson correlation matrix of RGB-derived vegetation indices under well-watered (WW) and induced drought (ID) conditions. (Positive correlations are shown in red and negative correlations in blue. The color intensity and circle size represent the strength of the correlation coefficient (r), ranging from –1 to +1).

PCA-based indices (PCA1, PCA2, IPCA) showed moderate correlations with several RGB-derived vegetation indices, underscoring their capacity to summarize multivariate spectral responses. Traits such as INT had lower correlations with other indices, indicating a limited contribution to genotype discrimination. Overall, the correlation analysis was effective in identifying groupings of co-responsive features for drought phenotyping.

Multi-trait genotype-ideotype distance index (MGIDI) analysis

The MGIDI analysis (Fig. 3) ranked the 28 genotypes based on their integrated RGB-derived vegetation indices under drought conditions. In this study, the ideotype configuration was defined using integrated RGB-derived vegetation indices, such that higher MGIDI values corresponded to genotypes exhibiting superior drought tolerance. Accordingly, genotypes such as G-23 (Queen Elizabeth), G-24 (Jwala), G-26 (Rosa chinensis), G-21 (Sylvia) and G-27 (Rose Sherbet) exhibited enhanced adaptive responses to drought stress. In contrast, genotypes including G-17 (*Rosa glutinosa)*, G-8 (*Rosa multiflora)*, G-12 (*Rosa brunonii)*, G-22 (*Rosa chinensis 'viridiflora')* and G-25 (*Rosa slancensis)* recorded lower MGIDI values, indicating greater sensitivity to drought stress.

Integration of leaf wilting score with RGB traits

Leaf wilting scores (LWS) varied significantly among genotypes under drought conditions, ranging from 0 to 5 (Fig. 4). No wilting symptoms were observed under WW conditions, confirming that LWS responded exclusively to induced drought stress. Genotypes such as G-21, G-23, G-26, G-2, G-24 and G-27 exhibited consistently low wilting scores (LWS ≤ 1), indicating superior maintenance of turgor and visual canopy integrity under water deficit condition. These observations complement RGB-derived vegetation indices and enhance the differentiation of genotypic responses to drought stress.

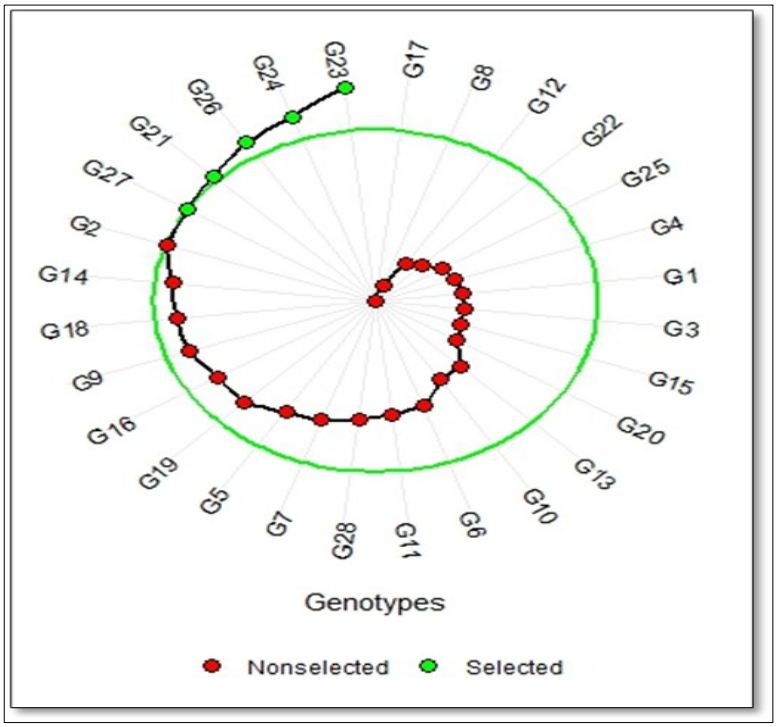

Fig. 3. Multi-Trait Genotype-Ideotype Distance Index (MGIDI) plot based on RGB-derived vegetation indices under well-watered (WW) and induced drought (ID) conditions in 28 rose genotypes.

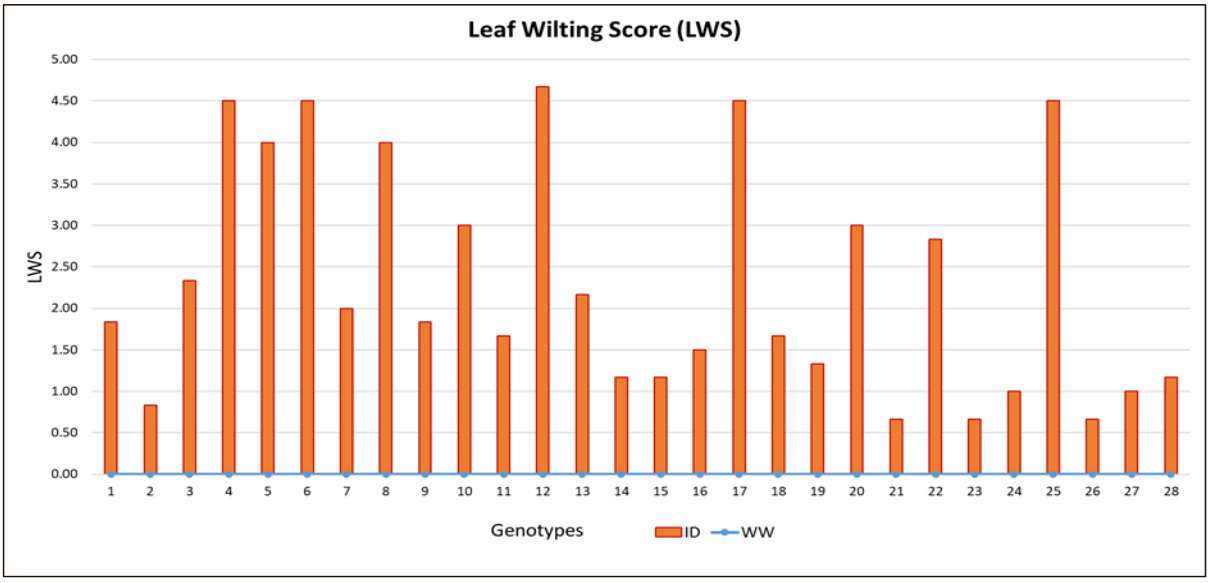

Fig. 4. Leaf Wilting Score (LWS) of 28 rose genotypes under well-watered (WW) and induced drought (ID) conditions.

Discussion

RGB-derived vegetation indices capture drought-responsive variation

The significant variation among the 28 rose genotypes across all the RGB-derived vegetation indices demonstrates the strong potential of RGB imaging to capture genotype-specific drought responses. The highly significant genotype × treatment (G × T) interactions observed in both side-view (SV) and top-view (TV) imaging indicate that genotypes differ markedly in brightness and canopy color under drought stress. These variations correspond to physiological processes such as reduced chlorophyll content, altered pigment composition and early senescence, reflecting inherent physiological and genetic differences in drought tolerance that were effectively quantified using RGB-based phenotyping. Similar drought-responsive behavior of RGB-derived vegetation indices has been reported in wheat (34), grapes (15), forage grasses (35) and pea and wheat (36), confirming their broad applicability across plant species.

Multi-angle imaging enhances trait detection

The distinct behavior of indices between SV and TV imaging emphasizes the importance of multi-angle phenotyping. In SV imaging, the highly significant interactions for basic RGB channels and their derived indices suggest strong sensitivity to drought-induced physiological changes such as chlorophyll decline, leaf folding and wilting. In contrast, green-blue indices such as NGBI_SV, GBRI_SV, GBVI_SV and b_SV showed moderate or lower significance, likely reflecting their weaker responsiveness to lateral canopy changes or reduced sensitivity to pigment shifts from this angle. TV imaging exhibited even stronger sensitivity to drought-related canopy changes, with nearly all indices showing highly significant G × T interactions. The top-view perspective captures the upper canopy, where early drought symptoms, such as reduced greenness, canopy thinning and pigment degradation are most evident. Only a few indices (RBRI_TV, RBVI_TV, NRBI_TV, PCA1_TV) showed moderate significance, indicating potential limitations of red –blue indices or PCA based indices, which may be less influenced by treatment effects, possibly due to inherent limitations in their sensitivity to subtle pigment changes in roses.

Overall, the strong and consistent G × T interactions observed across imaging perspectives demonstrate that RGB phenotyping effectively captured drought-responsive traits in rose. The top-view appears more informative for detecting drought-induced changes in leaf and canopy color, while the side-view provides complementary information from lateral canopy variations. This view-specific importance supports observations that multi-perspective imaging enhances phenotypic accuracy (37-39).

RGB imaging complements traditional scoring

The significant genotypic variation observed in Leaf Wilting Score (LWS) reflects physiological differences in drought tolerance among the rose genotypes. Genotypes with lower LWS exhibited higher greenness indices and lower red/blue reflectance-based indices, indicating healthier canopy condition under drought stress. These genotypes likely maintained higher leaf turgor, stronger root activity, or more efficient stomatal regulation, enabling them to delay visible wilting. The absence of wilting under well-watered conditions reaffirms LWS as a drought-specific indicator. Although LWS is a valuable measure, it is subjective, labor-intensive and less suitable for large-scale screening. In contrast, RGB imaging provides a sensitive, quantitative and high-throughput assessment of drought-induced changes in canopy color. The positive association between LWS and RGB-derived vegetation indices indicates that visual wilting assessments can be effectively supplemented or even replaced by high-resolution, non-destructive imaging methods (19). Genotypes such as G-21, G-23, G-26, G-2, G-24 and G-27, which maintained lower LWS (≤1), also ranked superior for RGB-derived vegetation indices, further validate the integration of traditional scoring with RGB phenotyping. Collectively, these findings highlight the potential of RGB-based phenotyping as a reliable proxy for LWS, reducing subjectivity and improving the efficiency and accuracy of drought tolerance screening in roses.

Multivariate analysis strengthens trait selection

PCA effectively separated vegetation indices based on physiological relevance. Greenness-related indices (e.g., ExG, g, RGBVI, Gray, GBVI, etc.) loaded strongly on PC1, affirming their association with chlorophyll content and canopy vigor. These indices are widely validated as indicators of biomass, photosynthetic capacity and plant health under stress conditions (40–44). In contrast, stress-reflectance indices (e.g., RGRI, RMBI, R, ExR, r, etc.) aligned along PC2 and showed enhanced reflectance due to pigment degradation during stress. The inclusion of PCA-derived composite indices (PCA1, PCA2, IPCA) further enabled dimensionality reduction while retaining key spectral information. This aligns with recent studies in forage grasses (35) that emphasize the utility of PCA in identifying core image-based traits responsive to environmental stress. The Pearson correlation matrix further strengthened these observations by revealing strong positive correlations ($r > 0.80$) among greenness indices and strong negative correlations ($r < –0.70$) among stress-reflectance indices. The MGIDI analysis efficiently integrated multi-trait RGB data into a single ranking index and produced a ranking framework for genotypes with higher adaptive features (45, 46). This confirms the utility of image-based MGIDI scoring as a comprehensive selection tool, aligning with breeding priorities and enabling high-throughput identification of drought-tolerant genotypes.

Conclusion

The findings highlighted RGB-based high-throughput phenotyping as a rapid, non-destructive and cost-effective method for screening drought tolerance in rose genotypes. Significant variation was observed across all 56 RGB-derived vegetation indices, with several key indices accurately reflecting changes in plant vigor and pigment degradation under stress. Multivariate analyses identified drought-tolerant genotypes, including ‘Queen Elizabeth’, ‘Jwala’, *Rosa chinensis*, ‘Sylvia’ and ‘Rose Sherbet’. Overall, RGB imaging offers a robust and scalable tool for accelerating drought screening in rose breeding programs.

Acknowledgements

All authors sincerely acknowledge the staff of the Floriculture and Landscaping Division, ICAR-IARI and Nanaji Deshmukh Plant Phenomics Centre, New Delhi, for their invaluable assistance during field experiments and image acquisition. We extend special thanks to Dr. Viswanathan Chinnusamy, In-charge of Phenomics, for his guidance and support, which greatly contributed to the successful execution of this research. This research was supported by the Indian Council of Agricultural Research, Department of Agricultural Research and Education, Government of India.

Authors' contributions

CK carried out the conceptualization, methodology design, project administration, data curation and prepared the original draft of the manuscript. N contributed to conceptualization, provided essential resources, conducted investigation and writing – review and editing. SK contributed to conceptualization, methodology development, provision of resources, supervision, software management and writing – review and editing. MKS and SP participated in methodology development, provision of resources and supervision. CB, AMS and BS contributed to methodology, validation and writing – review and editing. RR and V were responsible for formal analysis and visualization.

Compliance with ethical standards

Conflict of interest: Authors do not have any conflict of interest to declare.

Ethical issues: None

References

1. International Trade Centre (ITC). Trade Map: Trade statistics for international business development [Internet]. 2025 [cited 2025 Jun 10]. https://www.trademap.org
2. Leus L, Van Laere K, De Riek J, Van Huylenbroeck J, editors. Rose. In: Van Huylenbroeck J, editor. Ornamental crops. Cham: Springer; 2018. p. 719–67. https://doi.org/10.1007/978-3-319-90698-0_27
3. Datta SK. Rose. In: Rajasekaran T, editor. Floriculture and ornamental plants. Singapore: Springer Nature; 2022. p. 153–80. https://doi.org/10.1007/978-981-15-3518-5_8
4. Intergovernmental Panel on Climate Change (IPCC). Climate change 2021: the physical science basis. Contribution of Working Group I to the Sixth Assessment Report of the Intergovernmental Panel on Climate Change. Cambridge: Cambridge University Press; 2021.
5. Chaves MM, Maroco JP, Pereira JS. Understanding plant responses to drought—from genes to the whole plant. Funct Plant Biol. 2003;30:239–64. https://doi.org/10.1071/FP02076
6. Liao WB, Yu JH, Zhang ML. Drought resistance of nine ground cover rose cultivars. Acta Hortic. 2014;1035:125–34. https://doi.org/10.17660/ActaHortic.2014.1035.14
7. Al-Yasi H, Attia H, Alamer K, Hassan F, Ali E, Elshazly S, et al. Impact of drought on growth, photosynthesis, osmotic adjustment and cell wall elasticity in Damask rose. Plant Physiol Biochem. 2020;150:133–39. https://doi.org/10.1016/j.plaphy.2020.02.038
8. Bheemanahalli R, Gajanayake B, Lokhande S, Singh K, Seepaul R, Collins P, et al. Physiological and pollen-based screening of shrub roses for hot and drought environments. Sci Hortic. 2021;282:110062. https://doi.org/10.1016/j.scienta.2021.110062
9. Li L, Zhang Q, Huang D. A review of imaging techniques for plant phenotyping. Sensors. 2014;14:20078–111. https://doi.org/10.3390/s141120078
10. Singh A, Ganapathysubramanian B, Singh AK, Sarkar S. Machine learning for high-throughput stress phenotyping in plants. Trends Plant Sci. 2016;21:110–24. https://doi.org/10.1016/j.tplants.2015.10.015
11. Al-Tamimi N, Langan P, Bernád V, Walsh J, Mangina E, Negrão S. Capturing crop adaptation to abiotic stress using image-based technologies. Open Biol. 2022;12:210353. https://doi.org/10.1098/rsob.210353
12. Guo Y, Chen S, Wu Z, Wang S, Bryant CR, Senthilnath J, et al. Integrating spectral and textural information for monitoring growth of pear trees using optical images from the UAV platform. Remote Sens. 2021;13:1795. https://doi.org/10.3390/rs13091795
13. ElMasry G, Wang N, Vigneault C. Detecting chilling injury in Red Delicious apple using hyperspectral imaging and neural networks. Postharvest Biol Technol. 2009;52:1–8. https://doi.org/10.1016/j.postharvbio.2008.11.008
14. Selvaraj GM, Vergara A, Montenegro F, Ruiz HA, Safari N, Raymaekers D, et al. Detection of banana plants and their major diseases through aerial images and machine learning methods. ISPRS J Photogramm Remote Sens. 2020;169:110–24. https://doi.org/10.1016/j.isprsjprs.2020.08.025
15. Briglia N, Montanaro G, Petrozza A, Summerer S, Cellini F, Nuzzo V. Drought phenotyping in *Vitis vinifera* using RGB and NIR imaging. Sci Hortic. 2019;256:108555. https://doi.org/10.1016/j.scienta.2019.108555
16. Johansen K, Morton MJL, Malbeteau YM, Aragon B, Al-Mashharawi SK, Ziliani MG, et al. UAV-based phenotyping using morphometric and spectral analysis to quantify responses of wild tomato plants to salinity stress. Front Plant Sci. 2019;10:370. https://doi.org/10.3389/fpls.2019.00370
17. Gao G, Tester MA, Julkowska MM. The use of high-throughput phenotyping for assessment of heat stress-induced changes in Arabidopsis. Plant Phenomics. 2020;2020:1804651. https://doi.org/10.34133/2020/3723916
18. Enders TA, St Dennis S, Oakland J, Callen ST, Gehan MA, Miller ND, et al. Classifying cold-stress responses of inbred maize seedlings using RGB imaging. Plant Direct. 2019;3:e00104. https://doi.org/10.1002/pld3.104
19. Sarkar S, Ramsey AF, Cazenave AB, Balota M. Peanut leaf wilting estimation from RGB color indices and logistic models. Front Plant Sci. 2021;12:658621. https://doi.org/10.3389/fpls.2021.658621
20. Gamon JA, Surfus JS. Assessing leaf pigment content and activity with a reflectometer. New Phytol. 1999;143:105–17. https://doi.org/10.1046/j.1469-8137.1999.00424.x
21. Elshikha DEM, Hunsaker D, Bronson K, Sanchez P. Using RGB-based vegetation indices for monitoring guayule biomass, moisture content and rubber. In: Proceedings of the 2016 ASABE Annual International Meeting; 2016; Orlando (FL): American Society of Agricultural and Biological Engineers; 2016. p. 1–12.
22. Sellaro R, Crepy MA, Trupkin SA, Karayekov E, Buchovsky AS, Rossi C, et al. Cryptochrome as a sensor of the blue/green ratio of natural radiation in Arabidopsis. Plant Physiol. 2010;154:401–09. https://doi.org/10.1104/pp.110.160820
23. Baresel JP, Rischbeck P, Hu Y, Kipp S, Barmeier G, Mistele B, et al. Use of a digital camera for nondestructive detection of leaf chlorophyll and nitrogen status in wheat. Comput Electron Agric. 2017;140:25–33. https://doi.org/10.1016/j.compag.2017.05.032
24. Vincent L. Morphological grayscale reconstruction in image analysis: applications and efficient algorithms. IEEE Trans Image Process. 1993;2:176–201. https://doi.org/10.1109/83.217222
25. Kawashima S, Nakatani M. An algorithm for estimating chlorophyll content in leaves using a video camera. Ann Bot. 1998;81:49–54. https://doi.org/10.1006/anbo.1997.0544
26. Meyer GE, Hindman TW, Lakshmi K. Machine vision detection parameters for plant species identification. Proc SPIE. 1999;3543:327–35. https://doi.org/10.1117/12.336896
27. Meyer GE. Machine vision identification of plants. In: Ng TB, editor. Recent trends for enhancing the diversity and quality of soybean products. Rijeka: IntechOpen; 2011.
28. Woebbecke DM, Meyer GE, Von Bargen K, Mortensen DA. Color indices for weed identification under various soil, residue and lighting conditions. Trans ASAE. 1995;38:259–69. https://doi.org/10.13031/2013.27838
29. Sánchez-Sastre LF, Alte da Veiga NM, Ruiz-Potosme NM, Carrión-Prieto P, Marcos-Robles JL, Navas-Gracia LM, et al. Assessment of RGB vegetation indices to estimate chlorophyll content in sugar beet leaves. AgriEngineering. 2020;2:128–49. https://doi.org/10.3390/agriengineering2010009
30. Saberioon MM, Amin MSM, Anuar AR, Gholizadeh A, Wayayok A,

Khairunniza-Bejo S. Assessment of rice leaf chlorophyll content using visible bands at different growth stages. Int J Appl Earth Obs Geoinf. 2014;32:35–45.

31. Bendig J, Yu K, Aasen H, Bolten A, Bennertz S, Broscheit J, et al. Combining UAV-based plant height from crop surface models, visible and near infrared vegetation indices for biomass monitoring in barley. Int J Appl Earth Obs Geoinf. 2015;39:79–87. https://doi.org/10.1016/j.jag.2015.02.012
32. Gitelson AA, Kaufman YJ, Stark R, Rundquist D. Novel algorithms for remote estimation of vegetation fraction. Remote Sens Environ. 2002;80:76–87. https://doi.org/10.1016/S0034-4257(01)00289-9
33. Kazmi W, Garcia-Ruiz FJ, Nielsen J, Rasmussen J, Andersen HJ. Detecting creeping thistle in sugar beet fields using vegetation indices. Comput Electron Agric. 2015;112:10–19. https://doi.org/10.1016/j.compag.2015.01.008
34. Zhang L, Niu Y, Zhang H, Han W, Li G, Tang J, et al. Maize canopy temperature extracted from UAV thermal and RGB imagery and its application in water stress monitoring. Front Plant Sci. 2019;10:1270. https://doi.org/10.3389/fpls.2019.01270
35. De Swaef T, Maes WH, Aper J, Baert J, Cougnon M, et al. Applying RGB- and thermal-based vegetation indices from UAVs for high-throughput phenotyping of drought tolerance in forage grasses. Remote Sens. 2021;13:147. https://doi.org/10.3390/rs13010147
36. Zolin Y, Popova A, Yudina L, Grebneva K, Abasheva K, et al. RGB indices can be used to estimate NDVI, PRI and Fv/Fm in wheat and pea plants under drought and salinization. Plants. 2025;14:1284. https://doi.org/10.3390/plants14091284
37. Humplík JF, Lazár D, Husičková A, Spíchal L. Automated phenotyping of plant shoots using imaging methods for analysis of plant stress responses: a review. Plant Methods. 2015;11:29. https://doi.org/10.1186/s13007-015-0072-8
38. Briglia N, Williams K, Wu D, Li Y, Tao S, Corke F, et al. Image-based assessment of drought response in grapevines. Front Plant Sci. 2020;11:595. https://doi.org/10.3389/fpls.2020.00595
39. Wang S, Yang Y, Zeng J, Zhao L, Wang H, Chen S, et al. RGB imaging-based evaluation of waterlogging tolerance in cultivated and wild chrysanthemums. Plant Phenomics. 2025;7:100019. https://doi.org/10.1016/j.plaphe.2025.100019
40. Lussem U, Bolten A, Gnyp ML, Jasper J, Bareth G. Evaluation of RGB-based vegetation indices from UAV imagery to estimate forage yield in grassland. Int Arch Photogramm Remote Sens Spatial Inf Sci. 2018;42:1215–19. https://doi.org/10.5194/isprs-archives-XLII-3-1215-2018
41. Nehe AS, Foulkes MJ, Ozturk I, Rasheed A, York L, Kefauver SC, et al. Root and canopy traits and adaptability genes explain drought tolerance mechanisms in winter wheat. PLoS One. 2021;16:e0242472. https://doi.org/10.1371/journal.pone.0242472
42. Kazemi F, Parmehr EG. Evaluation of RGB vegetation indices derived from UAV images for rice crop growth monitoring. ISPRS Ann Photogramm Remote Sens Spatial Inf Sci. 2023;10:385–92. https://doi.org/10.5194/isprs-annals-X-4-W1-2022-385-2023
43. Wang Y, Yang Z, Kootstra G, Khan HA. Impact of variable illumination on vegetation indices and evaluation of illumination correction methods using UAV imagery. Plant Methods. 2023;19:51. https://doi.org/10.1186/s13007-023-01028-8
44. El-Hendawy S, Tahir MU, Al-Suhaibani N, Elsayed S, Elsherbiny O, Elsharawy H. Potential of thermal and RGB imaging combined with neural networks for assessing salt tolerance of wheat genotypes in field conditions. Agronomy. 2024;14:1390. https://doi.org/10.3390/agronomy14071390
45. Olivoto T, Nardino M. MGIDI: A novel multi-trait index for genotype selection in plant breeding. bioRxiv. 2020:2020.07.23.217778.
46. Al Mamun SA, Ivy NA, Khan MAI, Rehana S, Sultana MS, Adhikary SK, et al. Genotype selection from azide-induced rice mutants using multitrait genotype-ideotype distance index (MGIDI): Unveiling promising variants for yield improvement. Adv Agric. 2024;2024:5719580. https://doi.org/10.1155/2024/5719580

Additional information

Peer review: Publisher thanks Sectional Editor and the other anonymous reviewers for their contribution to the peer review of this work.

Reprints & permissions information is available at https://horizonepublishing.com/journals/index.php/PST/open_access_policy

Publisher's Note: Horizon e-Publishing Group remains neutral with regard to jurisdictional claims in published maps and institutional affiliations.

Indexing: Plant Science Today, published by Horizon e-Publishing Group, is covered by Scopus, Web of Science, BIOSIS Previews, Clarivate Analytics, NAAS, UGC Care, etc
See https://horizonepublishing.com/journals/index.php/PST/indexing_abstracting

Publisher information: Plant Science Today is published by HORIZON e-Publishing Group with support from Empirion Publishers Private Limited, Thiruvananthapuram, India.